Organic solar cells with carbon nanotube network electrodes

Michael W. Rowell,[a] Mark A. Topinka,[a),b)] and Michael D. McGehee[a)]
Department of Materials Science and Engineering, Stanford University, Stanford, California 94305

Hans-Jürgen Prall, Gilles Dennler, and Niyazi Serdar Sariciftci
Linz Institute for Organic Solar Cells (LIOS), Johannes Kepler University Linz, Altenbergerstrasse 69, A-4040 Linz, Austria

Liangbing Hu and George Gruner
Department of Physics and Astronomy, University of California, Los Angeles, Los Angeles, California 90093

(Received 14 March 2006; accepted 9 May 2006; published online 6 June 2006)

We fabricated flexible transparent conducting electrodes by printing films of single-walled carbon nanotube (SWNT) networks on plastic and have demonstrated their use as transparent electrodes for efficient, flexible polymer-fullerene bulk-heterojunction solar cells. The printing method produces relatively smooth, homogeneous films with a transmittance of 85% at 550 nm and a sheet resistance (R_s) of 200 $\Omega/\square$. Cells were fabricated on the SWNT/plastic anodes identically to a process optimized for ITO/glass. Efficiencies, 2.5% (AM1.5G), are close to ITO/glass and are affected primarily by R_s. Bending test comparisons with ITO/plastic show the SWNT/plastic electrodes to be far more flexible. © *2006 American Institute of Physics*. [DOI: 10.1063/1.2209887]

Organic and inorganic thin film solar cells are being pursued with much anticipation as viable alternatives to silicon solar cells, which dominate today's market.[1–3] A critical aspect of these solar cells is the current conduction across the illuminated side of the device in the transparent conductor (TC). The conventional anode of choice for organic solar cells has been indium tin oxide (ITO). However, high quality ITO is expensive, contains indium that might be too limited in supply for widespread use in solar energy applications, cannot be solution processed, and may not have the necessary flexibility for certain applications. These are critical barriers, as achieving commercial success will likely require the exploitation of key strengths, such as nonvacuum roll-to-roll-type manufacturing and opportunities in flexible applications. Recently an electronic material, a random carbon nanotube network film, has been explored[4,5] for applications where low sheet resistance (R_s) and high optical transparency (T) in the visible and infrared spectral range are essential. These films are made with solution processing, use abundant materials, and are highly flexible. Previous work has demonstrated the use of multiwalled carbon nanotube films as opaque organic solar cell anodes,[6] and more recently the use of single-walled carbon nanotube (SWNT) films as the transparent anode has been demonstrated on glass substrates.[7] However, in the latter case, T was low (~45% for R_s of 282 $\Omega/\square$) and the device configuration used an 800-nm-thick active absorber layer—thicker than is necessary to efficiently absorb sunlight.[8] Here, we have used a recently developed transfer-printing method[9] for producing SWNT transparent electrodes on flexible substrates. The method produces homogeneous, relatively smooth films, enabling the fabrication of conjugated polymer based bulk-heterojunction solar cells without the use of layers thicker than optimal. The SWNT films we have developed have T of 85% in the visible and R_s of 200 $\Omega/\square$. The achieved power efficiency of 2.5% (AM1.5G) approaches that of the control device made with ITO/glass (3%). Furthermore, the flexibility is far superior to devices using ITO coated on the same flexible substrate material.

A printing method, as described in detail earlier,[9] has been used to fabricate the transparent anode. Commercially available single-walled carbon nanotubes, produced by arc discharge, were dissolved in solution with surfactants and then sonicated. The well dispersed and stable solutions were vacuum filtered over a porous alumina membrane. Following drying, the SWNT films were lifted off with a poly(dimethylsiloxane) (PDMS) stamp and transferred to a flexible poly(ethylene terephthalate) (PET) substrate by printing. The density of this network (nanotubes/area) can be controlled with high precision by simply controlling the volume of dilute suspension filtered through the membrane. Our method also has the benefit that the speed of the vacuum filtering process does not allow for tube flocculation, creating homogeneous films, and the transfer-printing method produces relatively smooth films. Furthermore, the method is inexpensive, scalable to large areas, and allows for the transfer of the film to a variety of surfaces. The rms surface roughness of the networks was evaluated using an atomic force microscopy (AFM) probe and was found to be less than 10 nm over a surface of 25 μm^2. Figure 1(a) shows the homogeneity of the SWNT films.

The sheet conductance of the nanotube networks was evaluated with a two terminal method by subtracting the contact resistance between SWNT film and the metal contacts.[4] The transparency in the visible and infrared range (300–1100 nm) was measured by a Beckman Coulter DU 640 spectrophotometer. Figure 2 shows the wavelength dependence of the optical transparency of a 30-nm-thick network with 200 $\Omega/\square$ sheet resistance in the visible and infrared region. In contrast to ITO, for which a peak of the transparency is observed at 550 nm, the nanotube network retains high transparency towards the near IR part of the electromagnetic spectrum. One should note that in contrast to

[a)]Electronic mail: mmcgehee@stanford.edu
[b)]Also at Department of Physics, Stanford University, Stanford, CA 94305.

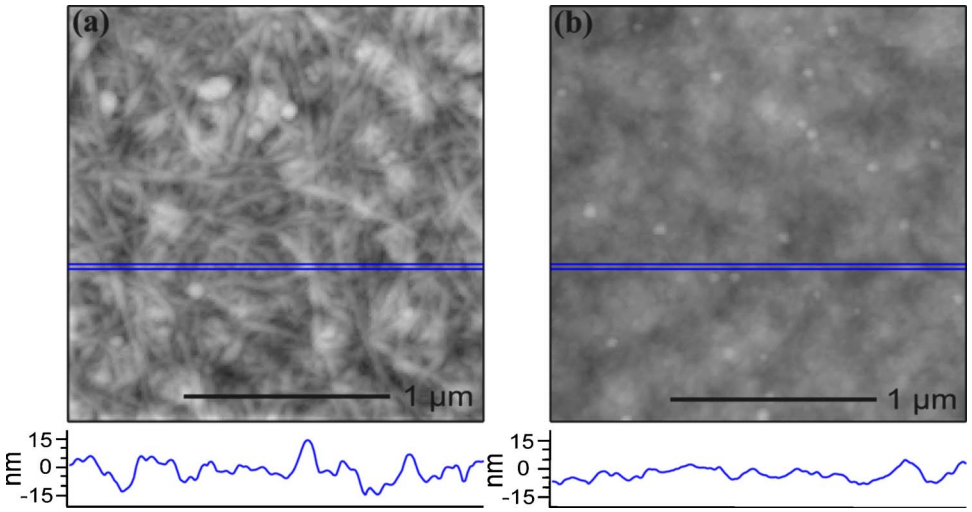

FIG. 1. (Color online) AFM images of SWNT network films (a) before and (b) after PEDOT:PSS deposition and annealing at 110 °C for 20 min. The rms roughness is 7 nm before coating and 3.5 nm after coating.

ITO, where T is mainly determined by the reflectance of the film, $T<100\%$ for SWNT films is due mainly to absorbance in the film.[9] The network can be tuned for an appropriate thickness, or density, and thus to an optimal optical transparency and sheet resistance. Consequently such networks, or films, can be used as transparent electrodes for a variety of applications. For solar cells, the optimal trade-off between T and R_s will vary depending on the intrinsic current-voltage characteristics of the device.

We have used 125-μm-thick PET flexible substrates coated with 30-nm-thick SWNT network films ($T=85\%$, $R_s=200\ \Omega/\square$) to fabricate solar cells with both poly[2-methoxy-5-(3′,7′-dimethyloctyloxy)-1,4-phenylene vinylene] (MDMO-PPV)/1-(3-methoxycarbonyl)-propyl-1-phenyl[6,6]C_{61} (PCBM) and poly(3-hexylthiophene) (P3HT)/PCBM.[10] Prior to depositing the active layer, a layer of poly(3,4-ethylenedioxythiophene):poly(styrene sulfonate) (PEDOT:PSS) was spin cast on the SWNTs at 1000 rpm and then placed directly on a 110 °C hot plate and annealed for 20 min. Consistent results were obtained when either the PEDOT:PSS solution was applied on the surface and let free to diffuse several minutes before the spin-coating operation in order to fill in the open porosity of the SWNT film or when a PEDOT:PSS/1:1 mix was used to improve the wetting. The PEDOT:PSS reduced R_s by approximately 20% to 160 $\Omega/\square$. The same PEDOT:PSS film spun on glass with no nanotubes (95 nm thick) had a sheet resistance of 15 k$\Omega/\square$, which is too high of a resistance to account for the drop in R_s simply due to parallel conduction. Therefore, two possible explanations are a reduction in the resistance between conducting nanotubes and/or doping of any semiconducting nanotubes. Figure 1(b) shows the SWNT films after being coated with PEDOT:PSS and the resulting low roughness. Samples were then transferred to an inert glovebox where a solution of MDMO-PPV/PCBM in a 1:4 weight ratio or P3HT/PCBM (Ref. 11) in a 1:0.8 weight ratio (10 mg P3HT/ml) in chlorobenzene was spin cast at 700 rpm. Finally, a 100 nm Al top electrode was evaporated under high vacuum at a rate of 0.1 nm/s. P3HT devices were annealed on a 120 °C hot plate for 10 min and had a postannealed optical density of 0.5. The overlap of the top and bottom electrodes defined a device of $1\times4\ \text{mm}^2$. The results are summarized in Table I for the flexible devices as well as a control device on ITO coated glass (15 $\Omega/\square$). The measured open circuit voltages (V_{oc}) suggest that, as proposed by Frohne *et al.*,[12] the V_{oc} is driven by the work function of the PEDOT:PSS layer rather than by the carbon nanotubes. Figure 3 shows the current-voltage curves for P3HT/PCBM cells under simulated AM1.5G conditions.

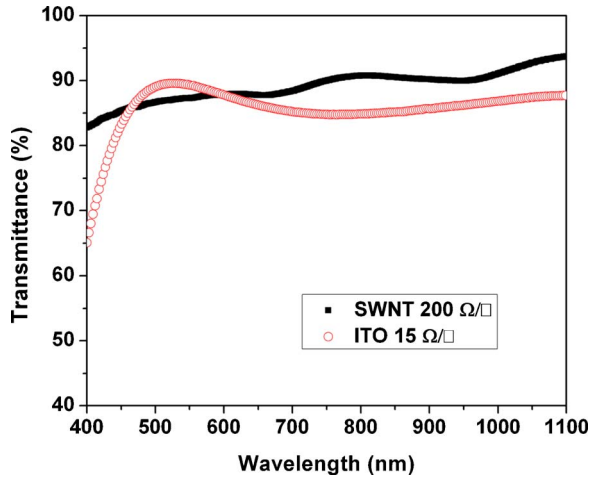

FIG. 2. (Color online) Transparency of a 30-nm-thick nanotube film with 200 $\Omega/\square$ sheet resistance, together with the transparency of ITO on glass (15 $\Omega/\square$).

The devices fabricated using SWNT networks operate almost identically to those for ITO coated glass with the exception of the fill factor (FF), which is likely attributable to the relatively high series resistance due to R_s. For solar cell applications, the TC must be as transparent and conductive as possible. The effect of the transparency is straightforward and the effect of the sheet resistance can be estimated to first order by Eq. (1), if the assumption is made that the voltage drop in the electrode is small enough that the current production is approximately homogeneous across the cell. For a cell of width w and length l, where current is collected at one of the edges with length l, the power loss (P_{loss}) due to R_s is given by (see, e.g., Goetzberger *et al.*[13])

$$P_{\text{loss}} = (jlw)^2 R_{\text{eff}}, \tag{1}$$

where $R_{\text{eff}}=R_s w/3l$. For example, to limit the fraction of power lost, $P_{\text{loss}}/(jlwV)$, to 10% for a cell with current density $j=8\ \text{mA/cm}^2$ and voltage $V=500$ mV at the maximum power point and $R_s=10\ \Omega/\square$, w must be less than 1.4 cm, and if $R_s=160\ \Omega/\square$, w is limited to 0.34 cm. For comparison, commercial Si solar cells typically have an emitter layer

TABLE I. Current density-voltage characteristics of devices under AM1.5G simulated illumination. (Oriel solar simulator, 100 mW/cm^2. A spectral mismatch factor of 1.25 was calculated using the measured photocurrent action spectra for our device and for the silicon photodiode, combined with the ideal AM1.5G spectrum and the actual spectrum produced by our simulator. Note that not including this factor would result in an approximately 20% overestimation of the efficiency of our devices.)

Device structure	j_{sc} (mA/cm^2)	V_{oc} (mV)	FF	Efficiency (%)
PET/SWNTs/PEDOT:PSS/MDMO-PPV:PCBM/Al	3.6	800	0.42	1.2
PET/SWNTs/PEDOT:PSS/P3HT:PCBM/Al	7.8	605	0.52	2.5
Glass/ITO/PEDOT:PSS/P3HT:PCBM/Al	8	610	0.61	3

with a sheet resistance of 40–100 Ω/□ (Ref. 14) with a current density of three to four times as much as today's organic solar cells. However, by screen printing thin contact fingers with $w \sim 0.2$ cm, losses from shadowing and R_s effects are kept to less than 10%.[13] For our P3HT:PCBM devices using SWNT/plastic anodes ($w=0.4$ cm, $j=5.8$ mA/cm^2, $V=430$ mV, and $R_s=160$ Ω/□), Eq. (1) predicts the fraction of power lost to be 12%. This agrees well with the observed loss of 17% using devices fabricated on ITO/glass anodes as the reference.

The stability of devices fabricated on the SWNT/PET films was much greater than devices on ITO/PET during simple bending tests. SWNT devices could be folded over (inducing compressive or tensile strain) down to radii of curvature of ~5 mm with no degradation in power efficiency and radii of ~1 mm with a 20%–25% loss in efficiency.

Interestingly, annealing for 5 min at 130 °C completely restored the efficiency in two out of three devices. The mechanisms involved in the failure or the restoration have not been investigated. In comparison, devices using ITO ($R_s=40$ Ω/□) on the same 125-μm-thick PET substrate began to fail at a radius of 1 cm and completely failed at 5 mm with fractures in the ITO visible to the eye.

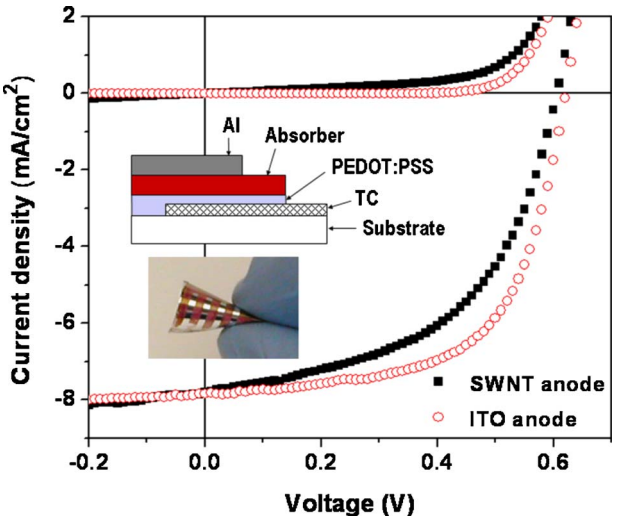

FIG. 3. (Color online) Current density-voltage characteristics of P3HT:PCBM devices under AM1.5G conditions using ITO on glass (open circles) and flexible SWNTs on PET (solid squares) as the anodes, respectively. Inset: Schematic of device and photograph of the highly flexible cell using SWNTs on PET.

These initial results suggest that with further optimization such anodes may offer a direct alternative to ITO and other transparent conducting oxides, in particular, under circumstances where mechanical flexibility is desirable. We have demonstrated before that the performance of transparent SWNT transistors remains virtually unchanged upon mechanical distortions[15] and here we have demonstrated that the efficiency of a working solar cell also is virtually unchanged. Furthermore, we believe that this represents only the beginning for the performance of SWNT TCs. Little has been done to investigate and control such effects as contact resistance between nanotubes, order of the nanotubes, doping, or use of only metallic nanotubes to name a few. The high mobility of individual nanotubes[16,17] indicates that significant improvement of the performance characteristics is possible through network optimization.

This work was supported in part by the Global Climate and Energy Project (GCEP) and NSF Grant No. DMR-040429.

[1] C. J. Brabec, J. A. Hauch, P. Schilinsky, and C. Waldauf, MRS Bull. **30**, 50 (2005).
[2] R. A. J. Janssen, J. C. Hummelen, and N. S. Sariciftci, MRS Bull. **30**, 33 (2005).
[3] P. Peumans, A. Yakimov, and S. Forrest, J. Appl. Phys. **93**, 3693 (2003).
[4] L. Hu, D. S. Hecht, and G. Gruner, Nano Lett. **4**, 2513 (2004).
[5] Z. C. Wu, Z. H. Chen, X. Du, J. M. Logan, J. Sippel, M. Nikolou, K. Kamaras, J. R. Reynolds, D. B. Tanner, A. F. Hebard, and A. G. Rinzler, Science **305**, 1273 (2004).
[6] H. Ago, K. Petritsch, M. S. P. Shaffer, A. H. Windle, and R. H. Friend, Adv. Mater. (Weinheim, Ger.) **11**, 1281 (1999).
[7] A. Du Pasquier, H. E. Unalan, A. Kanwal, S. Miller, and M. Chhowalla, Appl. Phys. Lett. **87**, 203511 (2005).
[8] K. M. Coakley and M. D. McGehee, Chem. Mater. **16**, 4533 (2004).
[9] Y. Zhou, L. Hu, and G. Gruner, Appl. Phys. Lett. **88**, 123109 (2006).
[10] G. Yu, J. Gao, J. C. Hummelen, F. Wudl, and A. J. Heeger, Science **270**, 1789 (1995).
[11] W. Ma, C. Yang, X. Gong, K. Lee, and A. J. Heeger, Adv. Funct. Mater. **15**, 1617 (2005).
[12] H. Frohne, S. E. Shaheen, C. J. Brabec, D. C. Muller, N. S. Sariciftci, and K. Meerholz, ChemPhysChem **3**, 795 (2002).
[13] A. K. Goetzberger, J. Knobloch, and B. Voss, *Crystalline Silicon Solar Cells* (Wiley, West Sussex, 1998), p. 110.
[14] V. Yelundur, K. Nakayashiki, M. Hilali, and A. Rohatgi, Proceedings of the 31st IEEE Photovoltaic Specialists Conference, Lake Buena Vista, FL, 3–7 January 2005, p. 959.
[15] E. Artukovic, M. Kaempgen, D. S. Hecht, S. Roth, and G. Gruner, Nano Lett. **5**, 757 (2005).
[16] T. Durkop, S. A. Getty, E. Cobas, and M. S. Fuhrer, Nano Lett. **4**, 35 (2004).
[17] J. Y. Park, S. Rosenblatt, Y. Yaish, V. Sazonova, H. Ustunel, S. Braig, T. A. Arias, P. W. Brouwer, and P. L. McEuen, Nano Lett. **4**, 517 (2004).